THE STRUCTURAL DESIGN OF TALL BUILDINGS, Vol. 5, 95–109 (1996)

SUCCESSFUL PERFORMANCE OF A BASE-ISOLATED HOSPITAL BUILDING DURING THE 17 JANUARY 1994 NORTHRIDGE EARTHQUAKE

MEHMET ÇELEBI†
USGS, Menlo Park, CA 94025, U.S.A.

SUMMARY

The purpose of this paper is to examine the response records and thereby the performance of the base-isolated University of Southern California (USC) hospital building during the $M_s = 6{\cdot}8$ Northridge (California) earthquake of 17 January 1994. The data retrieved from the building is the first set of data from any base-isolated building that (a) was tested to acceleration levels at the free-field similar to the zero period acceleration (ZPA) level postulated in the seismic design criteria of the building and (b) exhibits levels of relative displacement excursions which puts the isolators into the nonlinear range. The variation of the fundamental frequency as a function of changing instantaneous stiffness of the isolators is identifiable. During the shaking, the isolators (a) performed well and, having attained up to 10% hysteretic damping, effectively dissipated the incoming energy of motions and (b) reduced the drift ratios of the superstructure of the building to a maximum of 10% of the allowable, which should explain the fact that there was no damage to the structure or its contents. The primary conclusion of this study is that this base-isolated building performed well during the Northridge earthquake of 17 January 1994 when only approximately 10% of the displacement capability of the isolators were utilized. Therefore, there is every reason to believe that the building will perform well during future earthquakes in the region.

1. INTRODUCTION

Seismic isolation of structures is not new. During the last two decades, significant innovative applications of seismic isolation of structures have evolved. Laboratory tests of isolators have been conducted by many investigators including Kelly[1] and Çelebi and Kelly.[2] In the United States, California Division of Mines and Geology (CDMG), the United States Geological Survey (USGS) and other institutions have instrumented almost all of the base-isolated structures to record their responses during seismic events so that their performances can be evaluated.

The isolators change the dynamic characteristics of an otherwise fixed-base structure. The effective fundamental period of an isolated structure is typically 3–5 times longer than the same structure would have with a fixed base. Critical damping percentages of the isolators are, in general, greater than 10%. Therefore, a considerable percentage of the incoming seismic energy is dissipated by the isolators before being transmitted to the superstructure. The fact that the fundamental period lengthens has been a cause for concern and intensive discussion as to how such systems would respond to large ground displacements with long periods (approximately in

† Research Civil Engineer.

This article is a U.S. Government work and, as such, is in the public domain in the United States of America.

CCC 1062–8002/96/020095–15
© 1996 by John Wiley & Sons, Ltd.
Received January 1996
Revised February 1996

the 1–5 second range) typical of long-duration pulses generated by near-fault ground motions or surface wave motions of deep basins such as those in San Fernando and Los Angeles. Very recently, during the $M_s = 6{\cdot}8$ Northridge earthquake of 17 January 1994, the $M_s = 6{\cdot}7$ Erzincan (Turkey) earthquake of 13 March 1992 and the $M_s = 6{\cdot}7$ Kobe earthquake of 17 January 1995, the strong motions recorded exhibited such long duration pulses and intensified the discussion on the effect of these long-period motions on the performance of base-isolated (or other long-period) structures. Discussion of the issue of long duration pulses is beyond the scope of this paper (see Reference 3).

Until the 17 January 1994 Northridge (California) earthquake ($M_s = 6{\cdot}8$), the records obtained from a few base-isolated structures in the United States during prior events revealed that these buildings were not subjected to large enough motions to cause nonlinear displacement excursions of the isolators. However, during the 17 January 1994 Northridge earthquake, at 36 km from the epicenter, an impressive set of response records was retrieved by CDMG from the eight story base-isolated hospital building of the University of Southern California (USC) in Los Angeles.[8,12,17] To the knowledge of the author, these records are the first set of strong-motion records from a base-isolated structure where the free-field accelerations are at the level of ZPA postulated in its design criteria and the resulting displacements are large enough to show that the isolators experienced nonlinear displacement excursions and effectively reduced the peak accelerations and relative displacements of the superstructure. Furthermore, there was no damage to the building or its contents. On the other hand, the contents damage in another hospital complex within the vicinity of the USC hospital approached $400M (Colvin, see Reference 4).

Therefore, the purpose of this paper is to examine the response records and the performance of the base-isolated USC hospital which was tested to acceleration levels similar to the zero period acceleration (ZPA) postulated in the seismic design criteria of the building. The dynamic characteristics of the subject building are evaluated by two basic approaches: (a) spectral analyses; and (b) system identification techniques.[15] Finite element analyses of the building are not included in this study. At the time of writing of this paper, Nagarajah and Xiahong[5] also presented their findings, which are not contradictory to those presented herein.

2. THE BUILDINGS, ISOLATORS AND INSTRUMENTATION

The building is located in the north-east quadrant of the intersection of Highways 5 and 10 and is within 15 km of the Newport–Inglewood fault. The site is classified as a stiff soil (S1) site.[18] California Special Report 101 (Plate 1) shows the site as a rock outcrop (Puento formation—siltstone and sandstone).[13,14] Based on this, design response spectra of ATC-6 (same as UBC 1988 and 1994) for stiff soil type (S1) was adopted. The structure was designed to remain essentially elastic when subjected to seismic forces defined by an S1 spectrum with ZPA equal to $0{\cdot}4g$—increased by 20% to account for near field effects. This corresponds to the 'maximum probable earthquake' (MPE) ground motion with 10% probability of exceedence in 50 years. The foundation of the building is continuous concrete spread footings under the perimeter isolators and spread footings under interior isolators. The isolators are designed for a maximum 26 cm displacement. The clearance of the moat is approximately 33–35 cm (Asher *et al.*, see Reference 6).

A general three-dimensional view of the building and overall dimensions are seen in Figure 1. The steel superstructure of the building is supported by 149 isolators that are 34·6 cm (13·625 in high). The perimeter frames supported by 68 lead-rubber isolators that are 55·9 cm (22 in) square

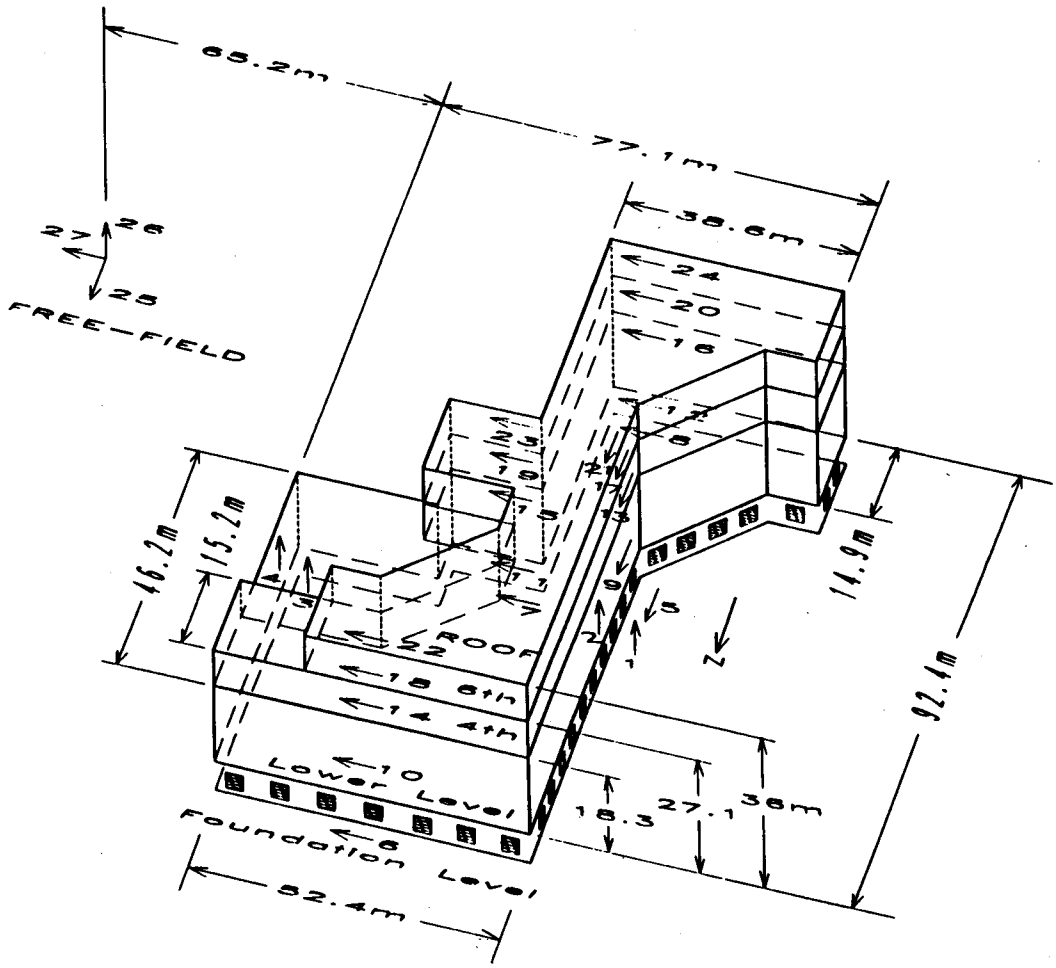

Figure 1. General three-dimensional schematic of the building: overall dimensions, the vertical and horizontal asymmetry and the instrumentation scheme are shown

are designed to carry the lateral loads and are diagonally braced. The internal vertical load carrying columns are supported by 81 elastomeric isolators that are 66·0 cm (26 in) square. The lower level diaphragm is a 25–37 cm (10–15 in) thick slab with 75–150 cm (2·5–5 ft) thick perimeter concrete beams. The upper floors slabs are 7·5–15 cm (3–6 in) thick on steel deck supported by steel beams (Asher *et al.*, see Reference 6).

Prototype isolators used in base-isolated structures are almost always tested in the laboratories. A sample plot of hysteresis loops generated during testing of a prototype lead–rubber isolator of the USC hospital is provided in Figure 2 (Mayes, see Reference 7). In the figure, three distinctive phases of stiffness are defined and will be used later in this paper. The figure also shows the maximum level of relative displacements experienced by the isolators. It is noted that the full displacement and dissipation capability of the isolators have not been exhausted during the earthquake.

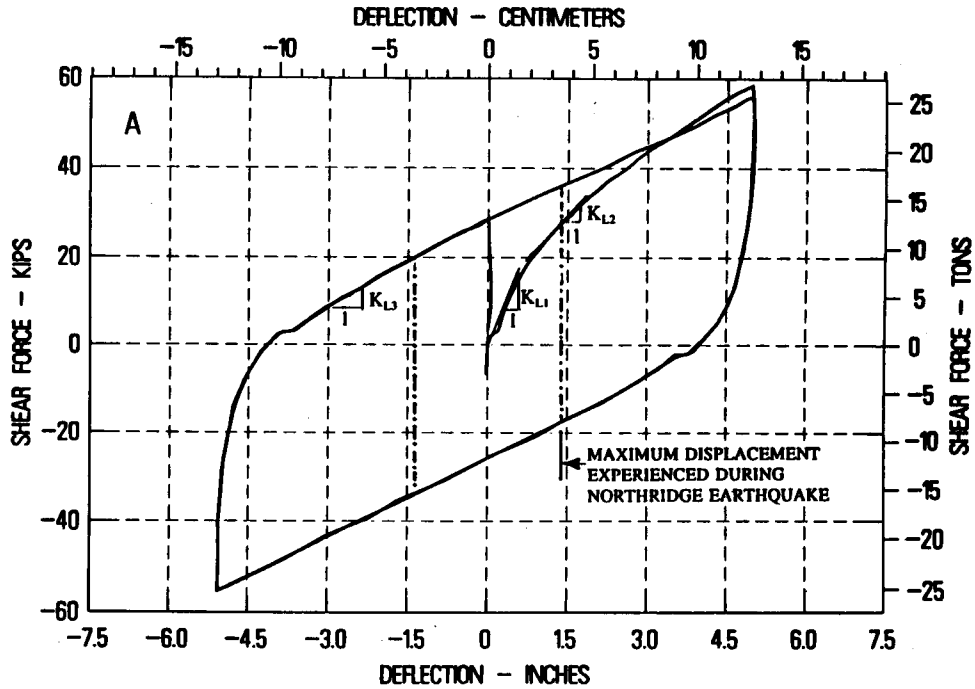

Figure 2. Hysteresis loops from the laboratory testing of a prototype lead–rubber isolator. Constant axial load during the test was 310 kips (141 tons) (Mayes, personal communication[7])

3. THE RECORDED DATA

The strong-motion instrumentation of the building as implemented by the California Strong-Motion Instrumentation Program of the State of California[8] comprises 24 unidirectional sensors within the building and 3 channels (triaxial) at the free-field site associated with the building. The instrumentation scheme, seen in Figure 1, is intended to record translational and torsional behavior of the superstructure as well as the foundation, the horizontal and vertical motions above and below the isolators, the diaphragm effect of the floor slabs and the free-field motions. The maximum peak accelerations of records (based-pass filtered with ramps at 0·1–0·2 and 46–50 Hz) at different levels of the building and at the free-field are summarized in Table I. The maximum peak accelerations in the EW direction were recorded in the south end of the

Table I. Variation of peak accelerations and displacements

Location	Max. peak accel. (g)			Max. peak displ. (cm)		
	NS	EW	UP	NS	EW	UP
Roof	0·21	0·19	—	3·9	5·1	—
6th Floor	0·11	0·15	—	3·3	4·0	—
4th Floor	0·10	0·16	—	3·1	3·3	—
Above isolators	0·13	0·14	0·10	2·8	3·0	1·3
Below isolators	0·37	0·17	0·09	1·7	2·3	1·4
Free-field	0·49	0·22	0·12	2·3	2·5	1·3

building, rightly so because that end is farthest away from center of rigidity of the building where the torsional contribution is largest. The fact that the larger horizontal peak acceleration in the free-field is 0·49*g* implies that the building was subjected to design level earthquake forces. Also noted from the table is that the free-field peak accelerations in either direction are larger than either the peak accelerations above the isolators or the roof—the first clear indication that the isolators dissipate the incoming vibrational energy and reduce the level of motions transmitted to the superstructure. It is noted that the acceleration levels increase significantly from the 6th floor to roof owing to drastic change in the plan of the building above the 6th floor.

4. ANALYSIS OF THE DATA

The acceleration and displacement time-histories are shown in Figure 3. Free-field response spectra (5% damped) of horizontal free-field motions are compared in Figure 4(a) with the UBC (S1) design response spectra scaled to 0·48*g*. The normalized free-field response spectra (5% damped) are compared in Figure 4(b) with those of the shape of the design response for UBC (or ATC) S1 soil type. In general, the shapes of the spectra of recorded components of motions appears to be well enveloped by the code spectrum except for some high frequency (>1 Hz) bands for which it is exceeded (at the specified spectral damping). It should be kept in mind that the free-field and foundation motions are transmitted to the superstructure through the isolators that attain greater than 10% damping. Therefore, there is no cause for alarm. Figures 4(c) and 4(d) show a comparison of 5% damped response spectra for locations at the roof, above and below isolators and free-field. Below 0·5 s, the roof spectrum is well below that of the free-field—showing that the isolators were effective.

The inevitable question is whether the isolators performed effectively. Figure 5 provides plots of relative accelerations recorded and calculated relative displacements above (AI) and below (BI) the isolators. In the NS direction, the maximum relative displacement is about 3·5 cm while in the EW direction, it is about 3·0 cm (at the south end). The magnitude of relative displacement excursions implies that the isolators experienced about 10% shear strain defined herein as the maximum relative displacement divided by the height of the isolators (34·6 cm). The amplitude spectra of these relative motions are shown in Figures 5(c) and 5(d), respectively, in which several close peaks indicate change of frequency during the response of the building. This will be explained further in the paper.

Roughly, from the hysteretic curves of Figure 2, this level of relative displacement corresponds to hysteretic damping of approximately 10%. The area within the hysteresis loops is proportional to the critical damping percentage (comparing the hysteretic area to the maximum elastic stored energy) by the relationship $d = \Delta(w)/4\pi(W)$ where $\Delta(w)$ is the actual area of the hysteresis loop at a displacement level and W is the hypothetical elastic energy defined by the area formed by the triangle with the line defining the elastic slope at the same displacement (see work by Hudson[9] and Jacobsen[10]). This level of damping is also confirmed by the system identification technique applied to the motions above isolators as output and below isolators as input and will be addressed later in the paper.

In Figure 6, time histories of velocity and relative cumulative energies (squared velocities summed up over time) of motions at free-field, below isolators, above isolators and the roof are shown. The nature of the incoming motions in the NS and EW directions (at free-field and below the isolators) are quite different. In the NS direction, a significant percentage of the incoming energy (approximately 50% within 1–2 s at about 16 s into the record, and 80% within 10 s of the record) impacts the structure. In the EW direction, approximately 80% of the energy comes in about 18 seconds mostly with approximately 3 s pulses. The isolators filter out the high

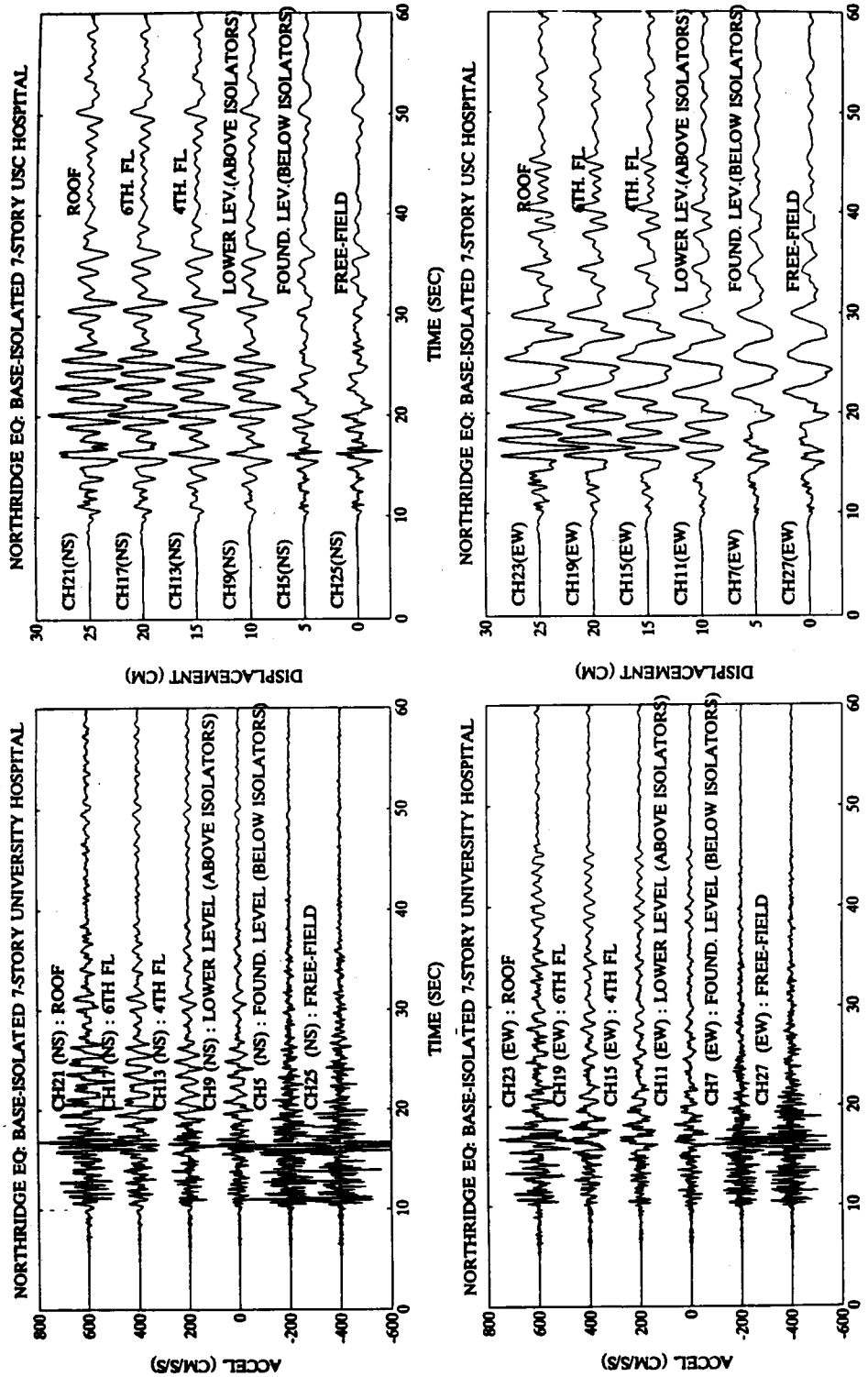

Figure 3. Acceleration and dispacement time-histories of motions recorded at different levels of the building, above and below the isolators and the free-field

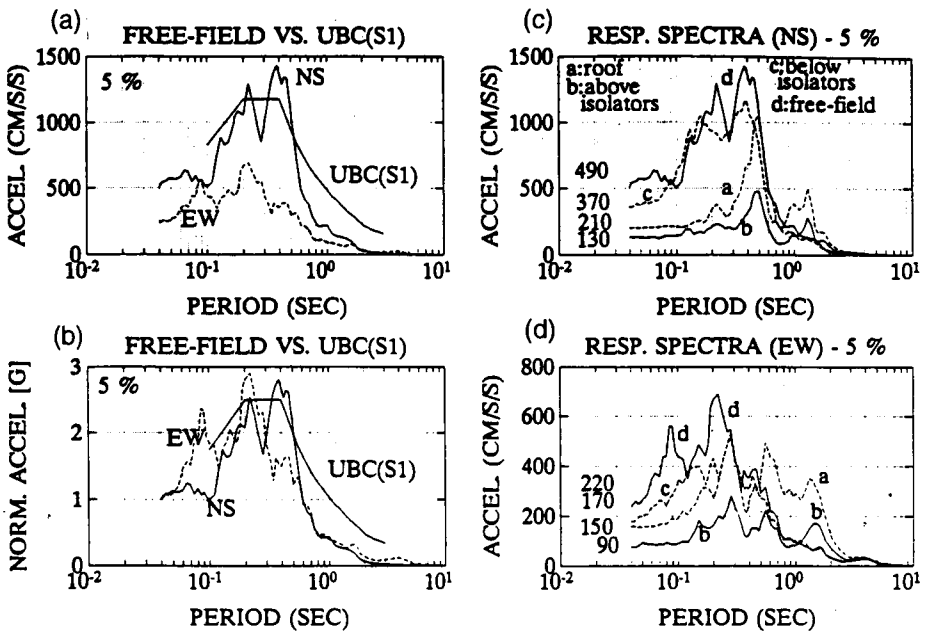

Figure 4. Comparison of (A) free-field spectra with design response spectra, (B) normalized to 1g, and (C) and (D) spectra of motions at different levels

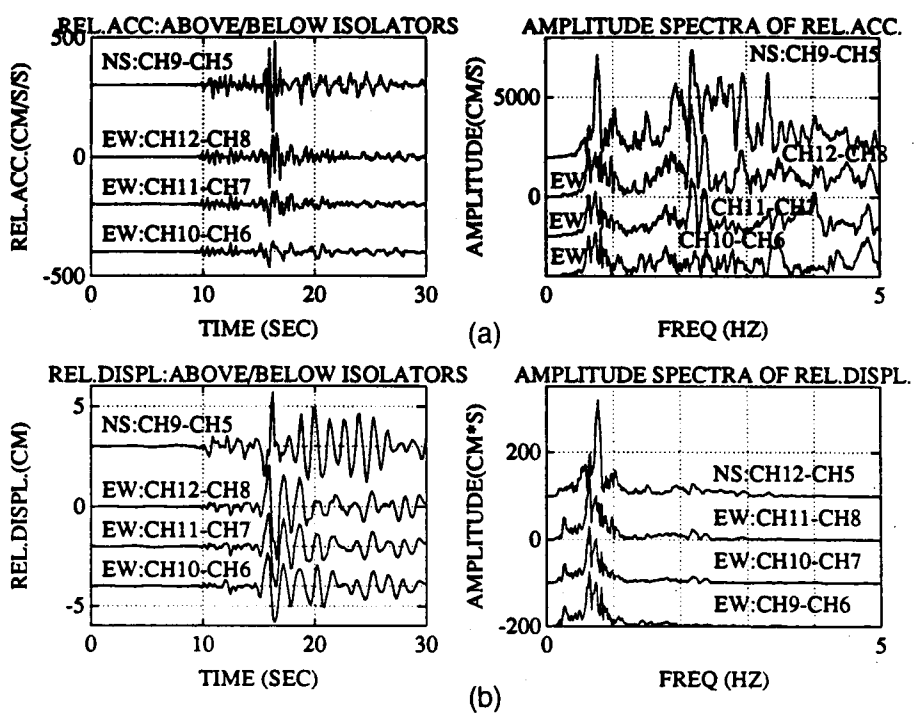

Figure 5. Relative (a) accelerations and (b) displacements calculated from motions recorded at (above, below) isolators and corresponding amplitude spectra

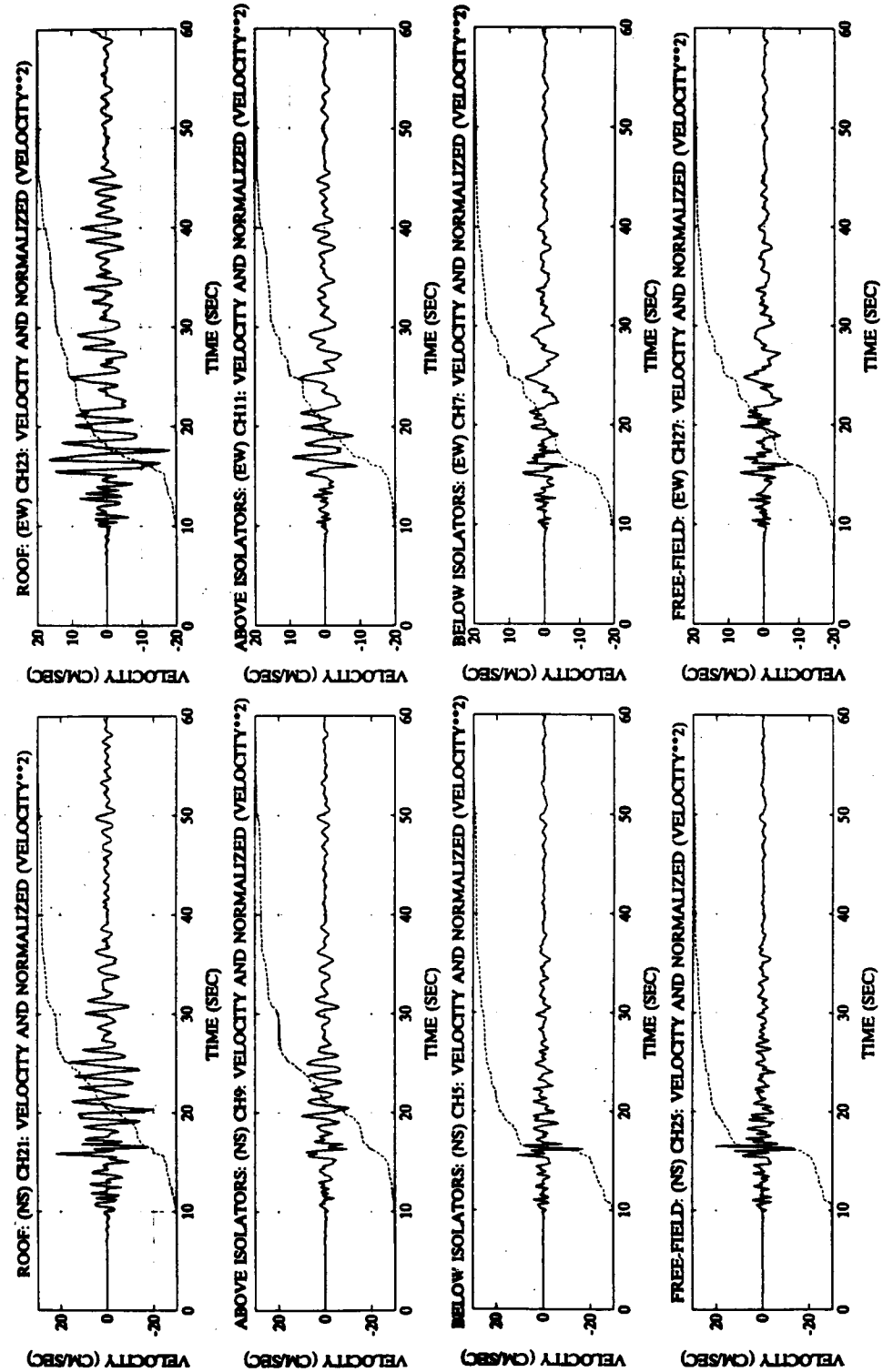

Figure 6. Cumulative relative energies using velocities at different levels

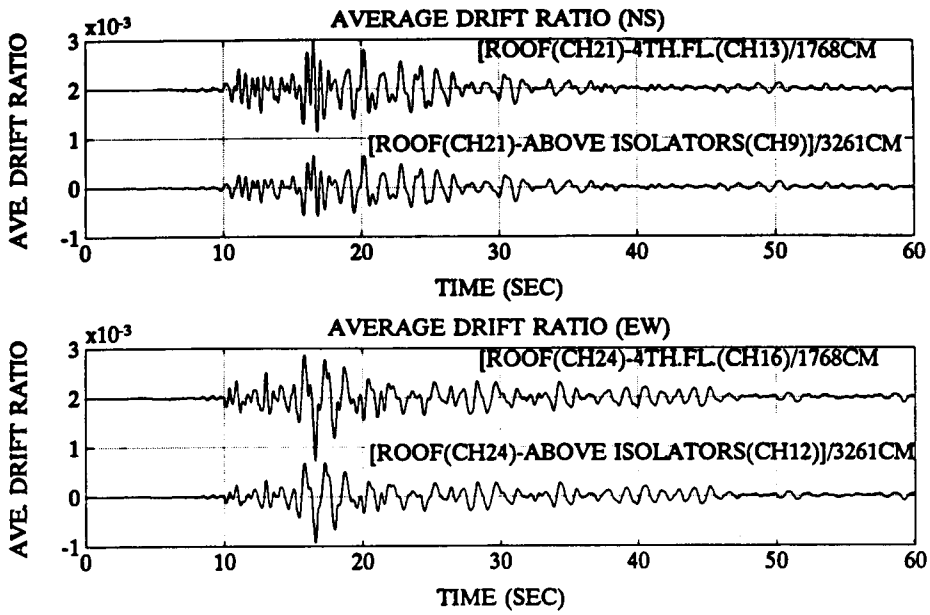

Figure 7. Drift ratios of the superstructure

frequency spike in the NS direction at about 16 s into the record and the vibrational energy above the isolators and the roof attains a relatively even rate.

Figure 7 shows the average drift ratio of the superstructure in the NS and EW directions computed from observed displacements at the roof, 4th floor and above the isolators. The average peak drift ratios are approximately 10% of the code allowable. The change in plan above the 4th floor does not increase the drift ratio, as evidenced by the average drift ratios between the roof and the 4th floor. It is concluded, therefore, that the isolators were effective in reducing the drift ratios of the superstructure.

Figures 8(a)–8(b) show the amplitude spectra computed using accelerations at the roof and the lower level above isolators (AI). There are distinctive peaks that can be identified within a band of frequencies as belonging to a specific mode of the vibrating building which is proof of the nonlinear (in this case, bi-linear) behavior of the isolators and its influence on the overall response of the building. For example, for the first mode, the frequencies are 0·7–0·75 and 1 Hz (NS) and 0·62 and 1 Hz (EW). To identify which frequency belongs to the fundamental mode and the second mode, Figures 8(g)–8(j) show the cross-spectra, coherence function and phase angle plots of the roof and 4th floor in the NS and EW directions, respectively. The 'family of frequencies' attributed to the first mode(s) seen in the cross-spectra are clearly in phase and have perfect coherence. Similarly, for the second mode (at 1·5–2 Hz), the motions are 180 deg out of phase at around 2 Hz and shifts in the frequencies are also clearly identifiable for that mode. At these identified frequencies, there is perfect coherence.

Figures 8(c)–8(d) show the amplitude spectra computed using accelerations at the foundation below isolators (BI) and the free-field. The amplitudes for BI are smaller than free-field, as were the peak accelerations. No definite site frequency can be identified from these spectra.

Figures 8(e)–8(f) show spectral ratios for the roof and BI (foundation level below isolators) for the NS and EW directions, respectively. These transfer functions show that the broad based structural peaks for frequencies less than 1 Hz.

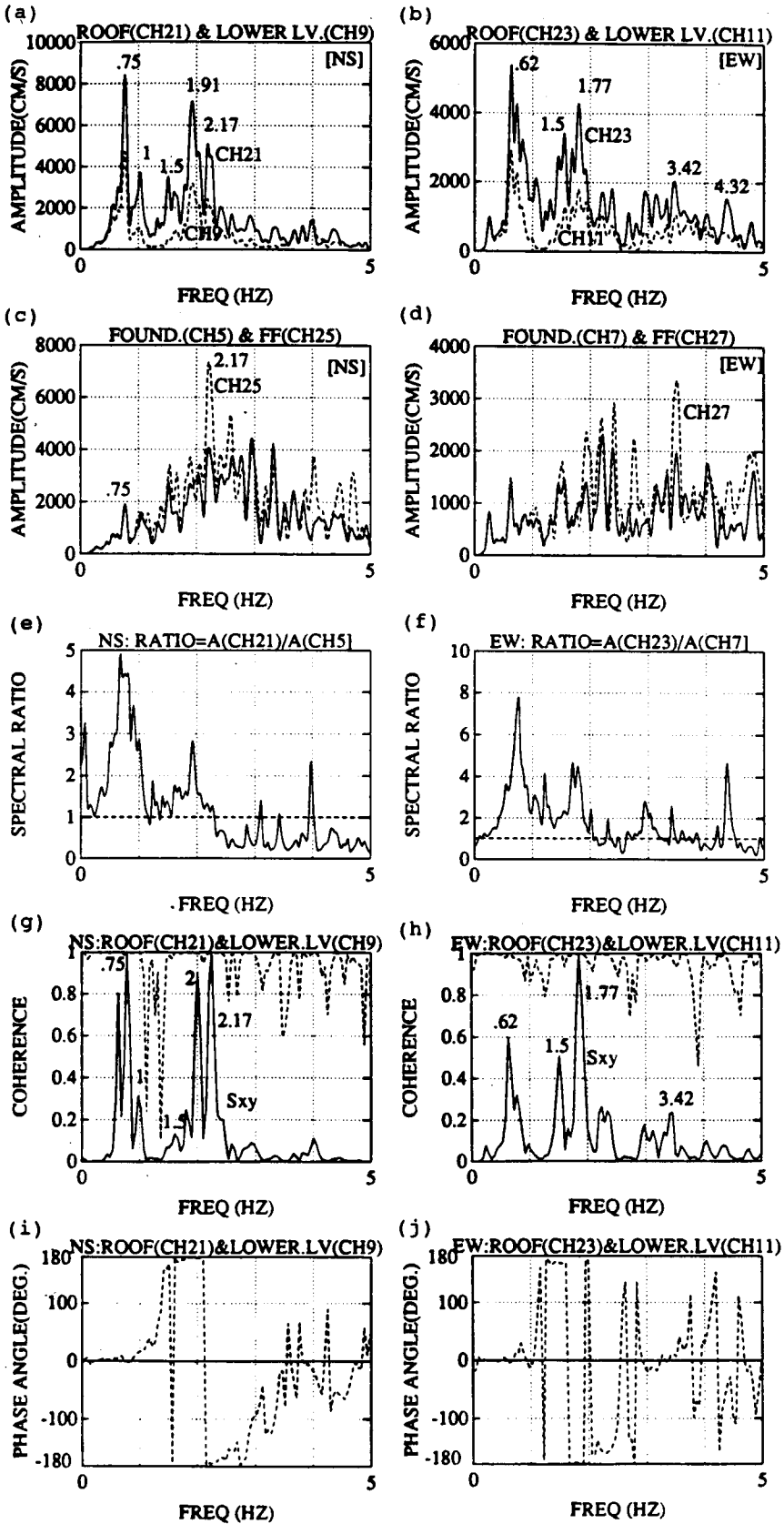
(a)
ROOF(CH21) & LOWER LV.(CH9)
[NS]
AMPLITUDE(CM/S)
.75
1
1.5
1.91
2.17
CH21
CH9
FREQ (HZ)
(b)
ROOF(CH23) & LOWER LV.(CH11)
[EW]
AMPLITUDE(CM/S)
.62
1.5
1.77
CH23
3.42
4.32
CH11
FREQ (HZ)
(c)
FOUND.(CH5) & FF(CH25)
[NS]
AMPLITUDE(CM/S)
.75
2.17
CH25
FREQ (HZ)
(d)
FOUND.(CH7) & FF(CH27)
[EW]
AMPLITUDE(CM/S)
CH27
FREQ (HZ)
(e)
NS: RATIO=A(CH21)/A(CH5)
SPECTRAL RATIO
FREQ (HZ)
(f)
EW: RATIO=A(CH23)/A(CH7)
SPECTRAL RATIO
FREQ (HZ)
(g)
NS:ROOF(CH21)&LOWER LV(CH9)
COHERENCE
.75
1
1.5
2
2.17
Sxy
FREQ (HZ)
(h)
EW:ROOF(CH23)&LOWER LV(CH11)
COHERENCE
.62
1.5
1.77
Sxy
3.42
FREQ (HZ)
(i)
NS:ROOF(CH21)&LOWER LV(CH9)
PHASE ANGLE(DEG.)
FREQ (HZ)
(j)
EW:ROOF(CH23)&LOWER LV(CH11)
PHASE ANGLE(DEG.)
FREQ (HZ)

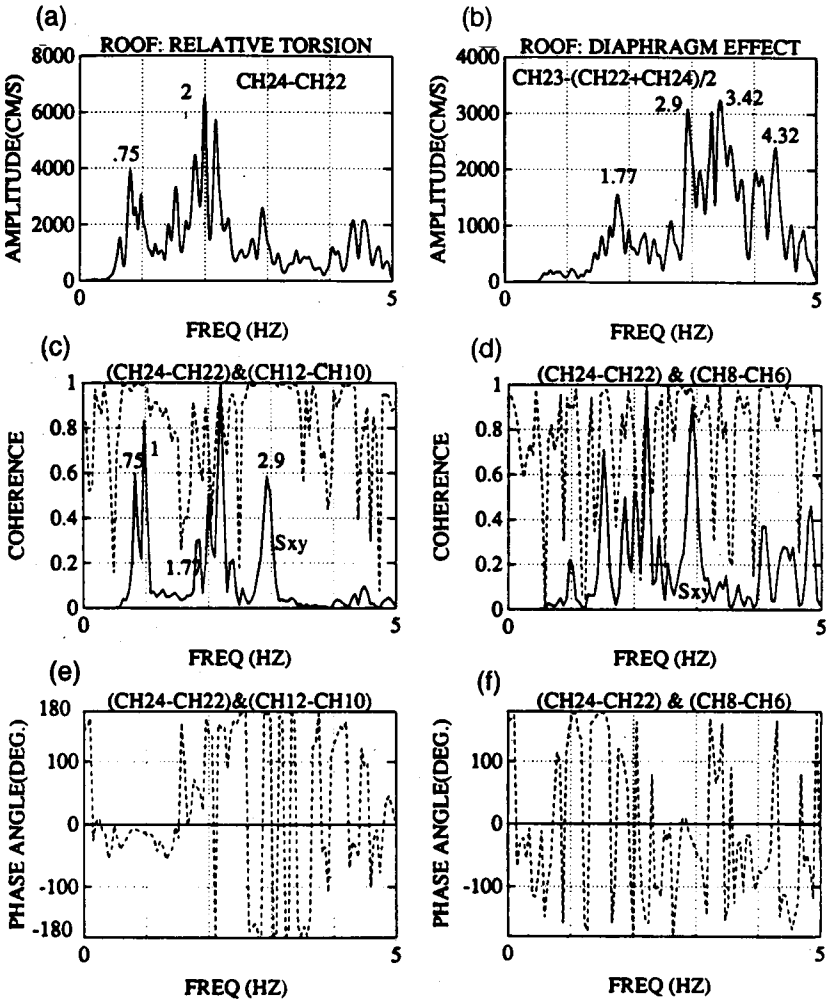

Figure 9. Amplitude spectra of (a) relative torsional accelerations and (b) accelerations to detect diaphragm effect, (c)–(f) coherence functions, cross-spectra and phase angles to distinguish torsional frequencies

Figure 9(a) shows the amplitude spectra for relative torsion at the roof. It is clearly seen that there is coupling of the translational and torsional modes. This is also confirmed by the fact that the torsional frequencies are the same as the translational frequencies, are coherent and are in phase for the first mode (0·75 and 1·0 Hz) and 180° degrees out of phase for the second mode (1·5–2 Hz). Figure 9(c)–9(f) depict these between the relative torsional acceleration between the roof and the lower level.

Figure 9(b) shows the amplitude spectrum to detect the diaphragm effect at the roof. The reason for several lumped-up frequency peaks at approximately 1·7, 3·4 and 4·2 Hz (also noted in the transfer functions) indicating the diaphragm effect may be due to the differences in diaphragm in-plane rigidities at different floors. However, at these higher frequencies, the diaphragm effect is not expected to contribute significantly to the overall response.

Figure 8. (a)–(d) Amplitude spectra of acceleration at different levels, (e)–(f) spectral ratios for roof and below isolators, (g)–(h) coherence functions and cross-spectra to distinguish several first and second translational modal frequencies and (i)–(j) phase angle plots

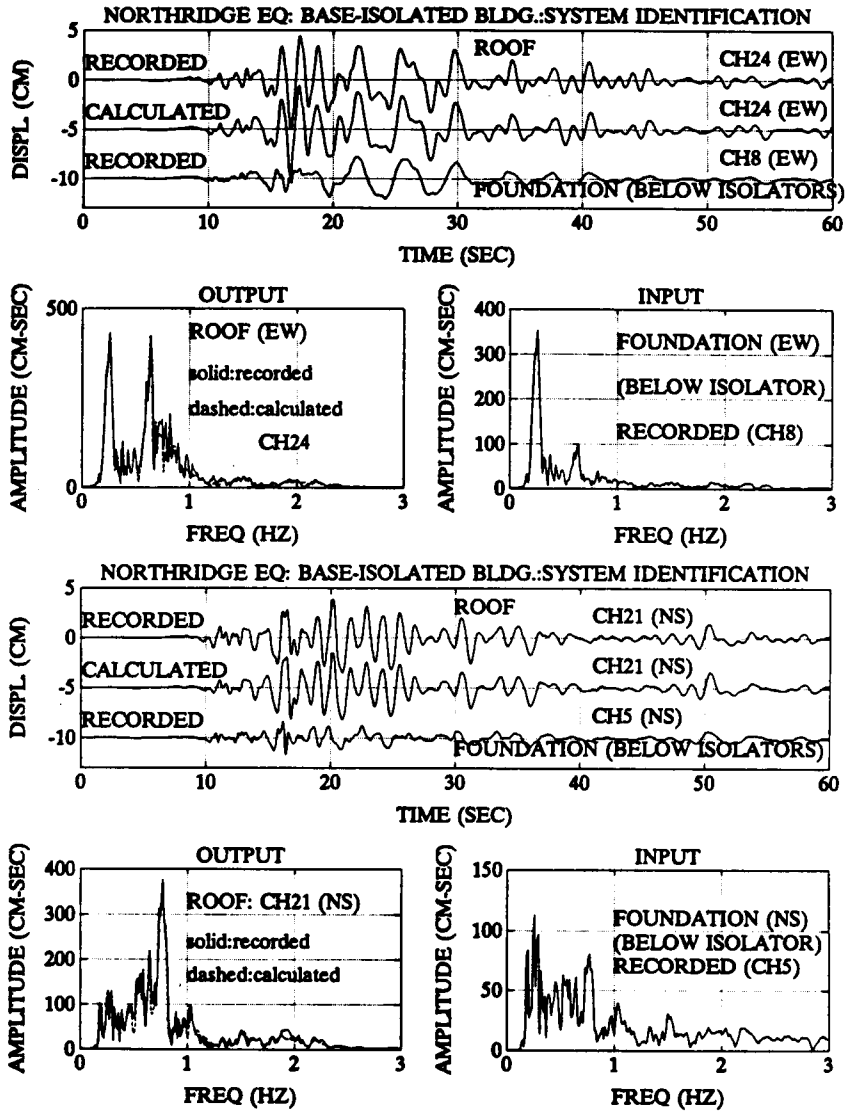

Figure 10. System identification of motions at the roof (output) and below isolators (input)

Figure 10 shows the results of system identification analyses applied to displacement records from the roof (output) and the basement below the isolators (input). Nonlinear effects were not incorporated in this effort. Simply, the ARX model based on the least squares method in the public domain program MATLAB was used.[15] From these, damping ratios of approximately 10 and 15% for the 1st and 2nd modes, respectively, are extracted. Essentially, the first mode dominates the response of the superstructure as seen in Figure 11, which shows that the displacement contributions of the first two modes as compared with the total displacement response.

It is important to note that the full displacement and dissipation capability of the isolators were only partially exhausted during the Northridge earthquake, suggesting that the performance

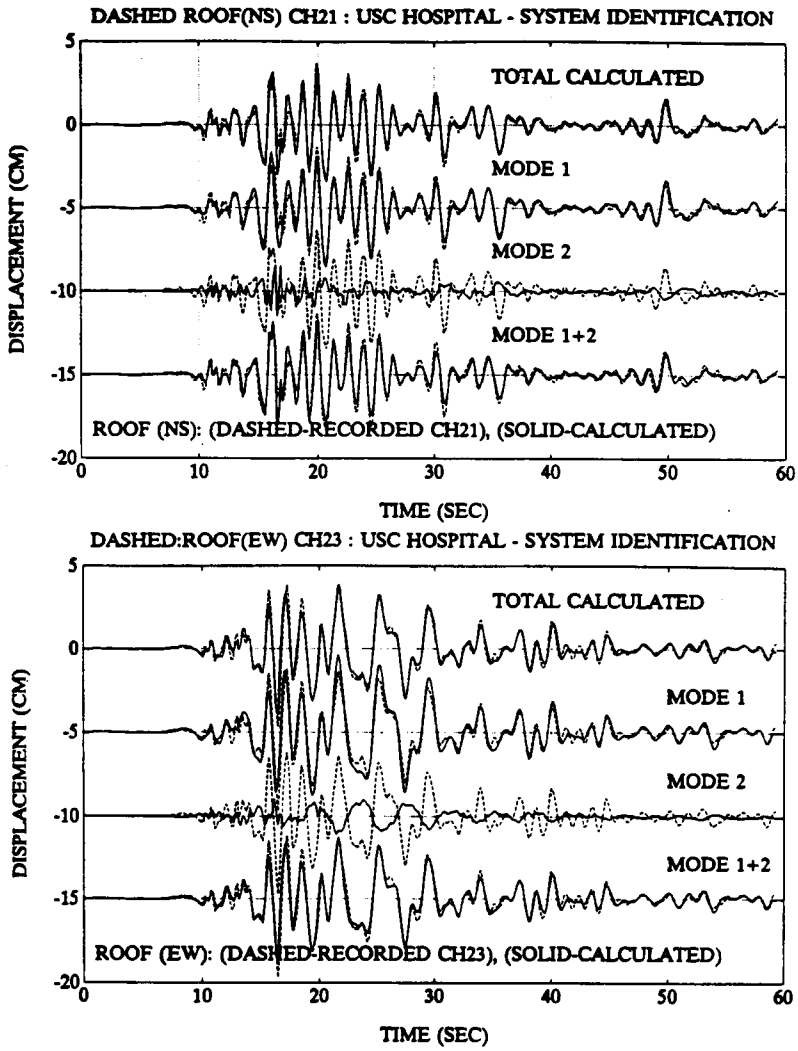

Figure 11. Displacement plots showing the first mode contributing most to the overall response

of the building and its isolators will be satisfactory during future events at possibly higher acceleration and displacement levels than those recorded at the site and experienced by the structure during the Northridge earthquake and compatible with the seismicity of the area. A detailed probabilistic evaluation of the seismic hazard in Southern California and probable earthquakes for a thirty year period (1994–2024) has been recently reassessed (Working Group[11]). Deliberations on this subject are beyond the scope of this paper.

However, it is possible to estimate the extreme situations for the building and its isolators with the known first mode frequency which starts at 1 Hz and then when nonlinear behavior of the isolators shifts to 0·7 Hz in the NS direction and similarly starts at 1 Hz and shifts to 0·62 Hz in the EW direction. For this, the stiffnesses for a bilinear hysteretic curve as defined by Asher *et al.*[12] are adopted. These stiffnesses, corresponding to 1 in (2·5 cm) displacement, are: $k_{L1} = 8{\cdot}55\ \mathrm{t\ cm^{-1}}$ for 59, and $9{\cdot}08\ \mathrm{t\ cm^{-1}}$ for 9, of the 68 lead–rubber isolators; and,

similarly, $k_{L2} = 1{\cdot}98$ t cm^{-1} for 59, and $2{\cdot}68$ t cm^{-1} for 9, lead–rubber bearings. The stiffnesses of the high damping rubber-only bearings are defined to be linear at 1 in (2·5 cm) and, therefore, $k_{R1} = k_{R2} = 2{\cdot}41$ t cm^{-1} for 8, and $3{\cdot}07$ t cm^{-1} for 73, of the 81 such bearings. To facilitate further evaluation at larger displacements, the author based on actual hysteresis plots for prototype isolators, extended these to $k_{L3} = 1$ t cm^{-1} for all lead–rubber bearings and $k_{R3} = 1{\cdot}75$ t cm^{-1} for all-rubber bearings. If the superstructure can be assumed to be rigid, and since the mass is constant, the fundamental frequency of the system at any displacement stage can be defined by $f_1 = (0{\cdot}5/\pi)(K_{1j}/M_{1j})^{0{\cdot}5}$ where $K_{1j} = 68k_{Li} + 81k_{Ri}$ is the total stiffness of the 68 lead and 81 rubber (=149) isolators. Thus, for the first mode only,

$$K_{11} = 59(8{\cdot}55) + 9(9{\cdot}08) + 8(2{\cdot}41) + 73(3{\cdot}07) = 830 \text{ t cm}^{-1}$$

$$K_{12} = 59(1{\cdot}98) + 9{\cdot}(2{\cdot}68) + 8(2{\cdot}41) + 73(3{\cdot}07) = 384 \text{ t cm}^{-1}$$

and

$$K_{13} = 68(1) + 81(1{\cdot}75) = 210 \text{ t cm}^{-1}$$

From these, equivalent mass units corresponding to the identified frequencies (1 and 0·7 Hz of the first mode are: $M_{11} = 21$ units (for $f_{11} = 1$ Hz and $K_{11} = 830$ t cm^{-1}) and $M_{12} = 19{\cdot}9$ units (for $f_{12} = 0{\cdot}7$ Hz and $K_{12} = 384$ t cm^{-1}). From this, an average equivalent mass is taken as $M_{1j} = 20$ units. Using this, the first mode frequency at large displacements can be estimated with K_{13}. Thus, at large displacements, $f_{13} \sim (0{\cdot}5/\pi)[210/20]^{0{\cdot}5} \sim 0{\cdot}46$ Hz (or approximately 2·2 s). At 2·2 s, the spectral accelerations are conservatively estimated from the free-field response spectrum of the Northridge earthquake with known low-frequency content to be less than 100 cm s^{-2}. Assuming an even higher spectral acceleration at 200 cm s^{-2}, the displacement of an isolator can then be estimated to be $d \sim S_a/w^2 \sim S_a/(2\pi f)^2 \sim 200/(2\pi[0{\cdot}46])^2 \sim 24$ cm, which is within the displacement capability of the isolators and less than the moat clearance.

In summary, the range of frequencies and damping for the USC hospital building are expected to be as summarized in Table II.

5. CONCLUSIONS

The primary conclusion of this study is that the base-isolated USC hospital building performed well during the Northridge earthquake of 17 January 1994 when the peak free-field acceleration was at a level comparable to the prescribed ZPA in its design criteria. The data from this building is the first set of data from any base-isolated building that exhibits excursions into the nonlinear range of the isolators. The drift ratios experienced by the superstructure are less than 10% of the allowable, which should explain that (a) there was no damage to the structure or its contents and (b) isolators performed well, reaching 10% hysteretic damping, effectively dissipating the

Table II. Range of effective frequencies (period) and damping percentages

	Frequency (Hz)	Period (sec)	Damping (%)
Mode	NS & EW	NS & EW	NS & EW
Translational 1	0·45–1·0	1–2·2	10–15
Translational 2	1·5–2·0	0·5–0·67	10–15
Torsional 1	0·45–1·0	1–2·2	—
Torsional 2	1·5–2·0	0·5–0·67	—

incoming energy of motions with accelerations levels equivalent to the design level accelerations. The variation of the fundamental frequency as a function of changing instantaneous stiffness of the isolators is identifiable. Furthermore, only approximately 10% of the displacement capability of the isolators was utilized during the Northridge earthquake, suggesting that the performance of the building and its isolators will be satisfactory during future events, which may generate acceleration and displacement levels compatible with the seismicity of the area and possibly be higher than those recorded at the site and experienced by the structure during the Northridge earthquake.

REFERENCES

1. J. Kelly, 'Seismic isolation, passive energy dissipation and active control', *Proc. ATC: 17-1 Seminar on State of the Art and State of Practice of Base Isolation*, 1993, Vol. 1, pp. 9–22.
2. M. Çelebi and J. Kelly, 'The implementation of seismic hazard reduction by base isolation', *Proc. 2nd Int. Conf. on Soil Dynamics and Earthquake Engineering.*
3. Scientists of the USGS and SCEC, 'The magnitude 6·7 Northridge, California, earthquake of 17 January 1994', *Science*, **266**, 389–397 (1994).
4. R. L. Colvin, 'Seismic design hailed for averting hospital damage', *Los Angeles Times*, 24 March 1994.
5. S. Nagarajaiah and S. Xiahong, 'Response of base isolated buildings during the 1994 Northridge earthquake', *Proc. Seminar on Seismological and Engineering Implications of Recent Strong-Motion Data (SMIP'95)*, California Strong Motion Instrumentation Program, Division of Mines and Geology, California Department of Conservation, 1995.
6. J. Asher, D. Van Volkinburg, R. Mayes, T. Kelly, B. Sveinsson and S. Hussain, 'Seismic isolation of the USC University Hospital', *Proc. 4th US National Conf. on Earthquake Engineering*, Palm Springs, California, U.S.A., 20–24 May, 1990, Vol. 3, pp. 529–538.
7. R. Mayes, Written personal communication, Dynamic Isolation Systems, Berkeley, CA, 1995.
8. A. Shakal, M. Huang, R. Darragh, T. Cao, R. Sherburne, P. Malhotra, C. Cramer, R. Sydnor, V. Graizer, G. Maldonado, C. Petersen and J. Wampole, 'CSMIP strong-motion records from the Northridge, California, earthquake of 17 January 1994', Report No. OSMS 94-07, California Department of Conservation, Sacramento, California, U.S.A., February 1994.
9. D. Hudson, 'Equivalent viscous friction for hysteretic systems with earthquake-like excitations', *Proc. IIIrd World Conf. on Earthquake Engineering*, New Zealand, 1965.
10. L. S. Jacobsen, 'Damping in composite structures', *Proc. IInd World Conf. on Earthquake Engineering*, Tokyo, Japan, 1960, pp. 1029–1040.
11. Working Group on the Probabilities of Future Large Earthquakes in Southern California, 'Seismic hazards in Southern California: Probable earthquakes, 1994–2024', *Bull. Seism. Soc. Am.*, **85**(2), 379–439 (1995).
12. J. Asher, S. Hosker, R. Ewing, D. Volkinburg, R. Mayes and M. Batton, 'Seismic performance of the base-isolated USC Hospital in the 1994 Northridge earthquake', *ASME/JSME Joint PVP Conf.*, Hawaii, U.S.A., 23–27 July, 1995, Vol. 319, pp. 147–154.
13. Tentative Provisions for the Development of Seismic Regulations for Buildings (ATC 3-06), Applied Technology Council, June 1978.
14. *Uniform Building Code (1988)*, Int. Conf. of Bldg. Officials (ICBO), Whittier, California, U.S.A.
15. *User's Manual: Main Program and System Identification Toolbox for Use with Matlab (1994)*, The Mathworks, Inc., South Natick, Massachusetts, U.S.A.
16. J. Kelly and M. Çelebi, 'Verification testing of prototype bearings for a base isolated building', Report UCB/SESM—84/01, University of California, Berkeley, California, U.S.A., March 1994.
17. Fact Sheet, USC University Hospital, DIS Inc., Berkeley, California, U.S.A.
18. D. L. Lamar, 'Geology of the Elysian Park–Repetto Hills Area, Los Angeles County, California', Plate 1 of Special Report 101, California Division of Mines and Geology, San Francisco, CA, 1970.